1971

Interaction equations for biaxially loaded sections, 1971 (72-9)

W. F. Chen

T. Atsuta

OFFICE

OF

RESEARCH

LEHIGH UNIVERSITY

Space Frames with Biaxial Loading in Columns

INTERACTION EQUATIONS FOR BIAXIALLY LOADED SECTIONS

by

W. F. Chen

T. Atsuta

Fritz Engineering Laboratory Report No. 331.17

INTERACTION EQUATIONS FOR BIAXIALLY LOADED SECTIONS

W. F. Chen[1] and T. Atsuta[2]

ABSTRACT

A simple method to obtain the exact interaction relationships of doubly symmetric sections under combined axial force and biaxial bending moments is presented. The exactness of the solution is proved by the coincidence of the upper and lower bound solutions provided by the limit analysis.

For illustration, interaction curves for a wide-flange section, a box section and a circular section are developed using the method.

Simple analytical expressions to approximate the interaction relations of wide-flange sections are proposed, and the associated plastic deformations are calculated.

[1]Associate Professor, Department of Civil Engineering, Lehigh University, Bethlehem, Pennsylvania.

[2]Engineer, Kawasali Heavy Industries, Ltd., Japan. Now a graduate student, Department of Civil Engineering, Lehigh University, Bethlehem, Pennsylvania.

1. INTRODUCTION

Biaxial interaction relationship of rectangular and wide-flange sections has been reported [1,2]. In Ref. 2, a procedure is presented for deriving approximate lower bound interaction equations in terms of axial force, torsional moment and biaxial bending moments. In Ref. 1, the accuracy of the solution was checked by the limit analysis, and the interaction relation was presented for the several different cases based on the location of the neutral axis. In that paper two Lagrange's multipliers were used to solve the variational problem in the case of the lower bound solution. Since the two multipliers have no specific physical meaning, the solutions derived in the several different cases could be verified only numerically.

Herein, two independent parameters with physical meanings are chosen. As a consequence, only one equation is needed for all possible cases and its exactness will be shown in what follows. This approach gives exact interaction relations and is applicable to any cross section doubly symmetrical.

Using the exact interaction relation, the ultimate strength of biaxially loaded columns could be found. In order to get an analytical solution, simple interaction equations are desired. This is done by curve fitting and it is found that interaction relations of wide-flange sections can be expressed by two simple equations with four constants which are dependent on the size of the section.

2. EXACT INTERACTION RELATIONS FOR A RECTANGULAR SECTION

Consider a rectangular section of width 2b and depth 2d as shown in Fig. 1. If the section is fully plastified, the normal stress can be assumed to be $-\sigma_y$ above the neutral axis (N.A.) and $+\sigma_y$ below the N.A. without loss of generality. Only axial stress is considered and the effect of shear stress on the yielding is neglected.

Location of the N.A. can be determined by two independent parameters: the vertical distance e and the angle with horizontal axis θ. The resultant forces of the section are obtained uniquely as functions of e and θ:

$$P = f_p\,(e,\theta): \text{ Axial force} \tag{1a}$$

$$M_x = f_x\,(e,\theta): \text{ Moment about horizontal axis} \tag{1b}$$

$$M_y = f_y\,(e,\theta): \text{ Moment about vertical axis} \tag{1c}$$

These functions are to be determined by the two limit analyses: the lower bound analysis and the upper bound analysis. The resulting functions, derived in the succeeding sections, are the same and hence exact.

2.1 Lower Bound Analysis

Since the state of stress given in Fig. 1 satisfies the yield condition and the equilibrium conditions, integration of stress over the section gives a lower bound solution for the biaxial bending forces.

The rectangular section can be divided into three parts: P-1, P-2 and P-3 by the neutral axis (N.A.) and a straight line N.B. as shown in Fig. 2. Lines N.B. and N.A. are symmetric with respect to the origin. From the symmetry with respect to both the x-axis and y-axis, the part P-2 contributes only to the axial force P and the parts P-1 and P-3 contribute only to bending moments M_x and M_y. The axial force P and the bending moment M_x and M_y are considered positive when the axial force causes tension and the bending moments produce compressive stress in the first quadrant of the coordinate system shown. Then the three resultant forces can be expressed as

$$P = \sigma_y A_2 \tag{2a}$$

$$M_x = \sigma_y A_1 e_{y1} + \sigma_y A_3 e_{y3} \tag{2b}$$

$$M_y = \sigma_y A_1 e_{x1} + \sigma_y A_3 e_{x3} \tag{2c}$$

where A_1, A_2 and A_3 are areas of parts P-1, P-2 and P-3, respectively, and e_{xj} and e_{yj} are the centroidal coordinates of portion P-j

$$(e_{x2} = e_{y2} = 0)$$

From symmetry again,

$$A_3 = A_1 \tag{3a}$$

$$e_{x3} = e_{x1} \tag{3b}$$

$$e_{y3} = e_{y1} \tag{3c}$$

Thus

$$A_2 = A - 2A_1 \tag{4}$$

where $A = 4bd$ is total area of the rectangular section.

Equations (2a), (2b) and (2c) become

$$P = \sigma_y A_2 = \sigma_y A_p \tag{5a}$$

$$M_x = 2\sigma_y A_1 e_{y1} = \sigma_y Q_x \tag{5b}$$

$$M_y = 2\sigma_y A_1 e_{x1} = \sigma_y Q_y \tag{5c}$$

where

$$A_p = A - 2A_1 \tag{6a}$$

$$Q_x = 2A_1 e_{y1} \tag{6b}$$

$$Q_y = 2A_1 e_{x1} \tag{6c}$$

In order to express A_1, e_{x1} and e_{y1} in terms of the two parameters e and θ, let us define a pair of parentheses which have the meaning

$$\langle S \rangle = \begin{cases} 0 & (S \leq 0) \\ S & (S \geq 0) \end{cases} \tag{7a}$$

or in a single expression

$$\langle S \rangle = \frac{S + |S|}{2} \tag{7b}$$

Considering the part P-1, there are three different cases possible as shown in Fig. 3. For each case, area and centroid can be obtained using the specially defined parentheses:

Part 4

$$A_4 = \frac{1}{2} \langle b \tan\theta + d - e \rangle^2 \cot\theta \tag{8a}$$

$$e_{y4} = \frac{1}{3} (-b \tan\theta + 2d + e) \tag{8b}$$

$$e_{x4} = \frac{1}{3} (2b \tan\theta - d + e) \cot\theta \tag{8c}$$

Part 5

$$A_5 = \frac{1}{2} \langle -b \tan\theta + d - e \rangle^2 \cot\theta \tag{9a}$$

$$e_{y5} = \frac{1}{3} (b \tan\theta + 2d + e) \tag{9b}$$

$$e_{x5} = \frac{1}{3} (2b \tan\theta + d - e) \cot\theta \tag{9c}$$

Part 6

$$A_6 = \frac{1}{2} \langle b \tan\theta - d - e \rangle^2 \cot\theta \tag{10a}$$

$$e_{y6} = \frac{1}{3} (b \tan\theta + 2d - e) \tag{10b}$$

$$e_{x6} = \frac{1}{3} (2b \tan\theta + d + e) \cot\theta \tag{10c}$$

and

$$A_1 = A_4 - A_5 - A_6 \tag{11a}$$

$$A_1 e_{x1} = A_4 e_{x4} + A_5 e_{x5} - A_6 e_{x6} \tag{11b}$$

$$A_1 e_{y1} = A_4 e_{y4} - A_5 e_{y5} + A_6 e_{y6} \tag{11c}$$

Equations (6a), (6c) and (6c) become

$$A_p = 4bd - \langle b \tan\theta + d - e \rangle^2 \cot\theta$$

$$+ \langle -b \tan\theta + d - e \rangle^2 \cot\theta \tag{12}$$

$$+ \langle b \tan\theta - d - e \rangle^2 \cot\theta$$

$$Q_x = \frac{1}{3} \langle b \tan\theta + d - e \rangle^2 \, (-b \tan\theta + 2d + e) \cot\theta$$

$$- \frac{1}{3} \langle -b \tan\theta + d - e \rangle^2 \, (b \tan\theta + 2d + e) \cot\theta \tag{13}$$

$$+ \frac{1}{3} \langle b \tan\theta - d - e \rangle^2 \, (b \tan\theta + 2d - e) \cot\theta$$

$$Q_y = \frac{1}{3} \langle b \tan\theta + d - e \rangle^2 \, (2b \tan\theta - d + e) \cot^2\theta$$

$$+ \frac{1}{3} \langle -b \tan\theta + d - e \rangle^2 \, (2b \tan\theta + d - e) \cot^2\theta \tag{14}$$

$$- \frac{1}{3} \langle b \tan\theta - d - e \rangle^2 \, (2b \tan\theta + d + e) \cot^2\theta$$

Define the non-dimensional forces as

$$p = \frac{P}{P_y} \;, \quad m_x = \frac{M_x}{M_{px}} \;, \quad m_y = \frac{M_y}{M_{py}} \tag{15}$$

in which

$$P_y = \sigma_y A \;, \quad M_{px} = \sigma_y Z_x \;, \quad M_{py} = \sigma_y Z_y \tag{16}$$

Therefore

$$p = \frac{A_p}{A} \;, \quad m_x = \frac{Q_x}{Z_x} \;, \quad m_y = \frac{Q_y}{Z_y} \tag{17}$$

in which

$$A = 4bd \quad \text{total area of the section} \tag{18a}$$

$$Z_x = 2bd^2 \quad \text{plastic section modulus about x-axis} \tag{18b}$$

$$Z_y = 2b^2d \quad \text{plastic section modulus about y-axis} \tag{18c}$$

The resultant forces p, m_x and m_y have now been expressed as functions of e and θ. The values of θ is valid in the region

$$0^\circ \leq \theta \leq 90^\circ \tag{19}$$

2.2 Upper Bound Analysis

An upper bound solution can be obtained by equating the internal rate of energy dissipation $\dot{D}_I$ due to an assumed strain field $\dot{\varepsilon}$ to the rates of external work $\dot{W}_E$ due to the increments of the resultant forces $\dot{P}$, $\dot{M}_x$ and $\dot{M}_y$.

Assume the rate of strain field as (Fig. 4)

$$\dot{\varepsilon} = - \eta \dot{\kappa} \tag{20}$$

in which η is the distance from fiber to the N.A.

The rate of internal dissipation is

$$\begin{aligned} \dot{D}_I &= \int_A \sigma \dot{\varepsilon} \, dA = \sigma_y \dot{\kappa} \left[\int_{A1} \eta \, dA - \int_{A2} \eta \, dA - \int_{A3} \eta \, dA \right] \\ &= \sigma_y \dot{\kappa} \, (\eta_1 A_1 + \eta_2 A_2 + \eta_3 A_3) \end{aligned} \tag{21}$$

in which η_i is the distance from the neutral axis N.A. to the centroids of the part P-i in η coordinate and

$$\eta_3 = 2\eta_2 + \eta_1 \quad , \quad A_3 = A_1 \tag{22}$$

From Fig. 5, η_1 and η_2 are related to e, θ, e_{x1} and e_{y1} as

$$\begin{aligned} \eta_1 &= e_{x1} \sin \theta + e_{y1} \cos \theta - e \cos \theta \\ \eta_2 &= e \cos \theta \end{aligned} \tag{23}$$

and the dissipation becomes

$$\begin{aligned} \dot{D}_I &= \sigma_y \dot{\kappa} [2\eta_1 A_1 + (2A_1 + A_2) \eta_2] \\ &= \sigma_y \dot{\kappa} (2A_1 e_{x1} \sin \theta + 2A_1 e_{y1} \cos \theta + A_2 e \cos \theta) \end{aligned} \tag{24}$$

The rate of external work is

$$\dot{W}_E = \dot{\epsilon}_o P + \dot{\kappa}_x \dot{M}_x + \dot{\kappa}_y M_y \tag{25}$$

where

$$\dot{\epsilon}_o = \text{strain rate at the centroid 0} \tag{26a}$$

$$\dot{\kappa}_x = \text{curvature rate about x-axis} \tag{26b}$$

$$\dot{\kappa}_y = \text{curvature rate about y-axis} \tag{26c}$$

and

$$\dot{\epsilon}_o = \dot{\kappa} e \cos \theta \tag{27a}$$

$$\dot{\kappa}_x = \dot{\kappa} \cos \theta \tag{27b}$$

$$\dot{\kappa}_y = \dot{\kappa} \sin \theta \tag{27c}$$

Then

$$\dot{W}_E = \dot{\kappa}\ (P\ e \cos\theta + M_x \cos\theta + M_y \sin\theta) \tag{28}$$

Equating the rate of internal energy dissipation to the rate of external work, $\dot{W}_E = \dot{D}_I$, one obtains

$$\begin{aligned} &P\ e \cos\theta + M_x \cos\theta + M_y \sin\theta \\ &= \sigma_y\ (A_2\ e \cos\theta + 2A_1\ e_{y1} \cos\theta + 2A_1\ e_{x1} \sin\theta) \end{aligned} \tag{29}$$

Equation (29) must be valid for all values of e and θ. It follows that

$$\begin{aligned} P &= \sigma_y\ A_2 \\ M_x &= 2\sigma_y\ e_{y1}\ A_1 \\ M_y &= 2\sigma_y\ e_{x1}\ A_1 \end{aligned} \tag{30}$$

which is identical to Eq. (5) obtained from lower bound analysis. Therefore, it can be concluded that the solution is exact.

3. EXACT INTERACTION RELATIONS FOR DOUBLE WEB SECTIONS

A double web section as shown in Fig. 6 is a general case, and Eqs. (12), (13), (14) and (18) can be extended to the general case. The function A_p for the general case, for example, can be obtained by first finding the functions $A_p\ (b_o, d_o)$, $A_p\ (b_o, d_1)$, $A_p\ (b_1, d_1)$, and $A_p\ (b_2, d_1)$ corresponding to the rectangular sections $2b_o \times 2d_o$, $2b_o \times 2d_1$, $2b_1 \times 2d_1$, and $2b_2 \times 2d_1$, respectively. The function A_p for the double web section is then obtained by the simple algebraic summation,

$$A_p = A_p(b_o,d_o) - A_p(b_o,d_1) + A_p(b_1,d_1) - A_p(b_2,d_1) \tag{31a}$$

similarly,

$$Q_x = Q_x(b_o,d_o) - Q_x(b_o,d_1) + Q_x(b_1,d_1) - Q_x(b_2,d_1) \tag{31b}$$

$$Q_y = Q_y(b_o,d_o) - Q_y(b_o,d_1) + Q_y(b_1,d_1) - Q_y(b_2,d_1) \tag{31c}$$

$$A = 4\,(b_o d_o - b_o d_1 + b_1 d_1 - b_2 d_1) \tag{32a}$$

$$Z_x = 2\,(b_o d_o^2 - b_o d_1^2 + b_1 d_1^2 - b_2 d_1^2) \tag{32b}$$

$$Z_y = 2\,(b_o^2 d_o - b_o^2 d_1 + b_1^2 d_1 - b_2^2 d_1) \tag{32c}$$

Particular cases may then be handled using these equations and the special properties in each case.

<u>Rectangular Section (B x D)</u>

$$\begin{aligned} b_o &= \frac{1}{2} B \;, \quad b_1 = \frac{1}{2} B \;, \quad b_2 = 0 \\ d_o &= \frac{1}{2} D \;, \quad d_1 = 0 \end{aligned} \tag{33}$$

<u>Box Section (B x D, t_f, t_w)</u>

$$\begin{aligned} b_o &= \frac{1}{2} B \;, \quad b_1 = \frac{1}{2} B \;, \quad b_2 = \frac{1}{2} B - t_w \\ d_o &= \frac{1}{2} D \;, \quad d_1 = \frac{1}{2} D - t_f \end{aligned} \tag{34}$$

<u>Wide-Flange Section (B x D, t_f, t_w)</u>

$$\begin{aligned} b_o &= \frac{1}{2} B \;, \quad b_1 = \frac{1}{2} t_w \;, \quad b_2 = 0 \\ d_o &= \frac{1}{2} D \;, \quad d_1 = \frac{1}{2} D - t_f \end{aligned} \tag{35}$$

4. EXACT INTERACTION RELATIONS FOR A CIRCULAR SECTION

Consider a solid circular section of radius r as shown in Fig. 7. The neutral axis (N.A.) is at a distance e from the center and makes an angle θ with x-axis. The part P-1 above the N.A. is assumed fully stressed by σ_y. Area and centroid of this portion are given by

$$A_1 = r^2 \left(\varphi - \frac{1}{2} \sin 2\varphi\right) \tag{36a}$$

$$e_{x1} = \frac{1}{2} r \sin\theta \, \frac{\sin\varphi - \frac{1}{3}\sin 3\varphi}{\varphi - \frac{1}{2}\sin 2\varphi} \tag{36b}$$

$$e_{y1} = \frac{1}{2} r \cos\theta \, \frac{\sin\varphi - \frac{1}{3}\sin 3\varphi}{\varphi - \frac{1}{2}\sin 2\varphi} \tag{36c}$$

where

$$\varphi = \cos^{-1} \frac{\bar{e}}{r} \tag{37a}$$

$$\frac{\bar{e}}{r} = \begin{cases} \frac{e}{r} & (\frac{e}{r} \leq 1) \\ 1 & (\frac{e}{r} \geq 1) \end{cases} \tag{37b}$$

or

$$\frac{\bar{e}}{r} = 1 - \left\langle 1 - \frac{e}{r} \right\rangle \tag{38}$$

and the corresponding quantities are derived as

$$A_p(r) = A - 2A_1 = \pi r^2 - 2r^2 \left(\varphi - \frac{1}{2}\sin 2\varphi\right) \tag{39a}$$

$$Q_x(r) = 2A_1 e_{y1} = r^3 \cos\theta \left(\sin\varphi - \frac{1}{3}\sin 3\varphi\right) \tag{39b}$$

$$Q_y(r) = 2A_1 \; e_{x1} = r^3 \sin\theta \left(\sin\varphi - \frac{1}{3}\sin 3\varphi\right) \tag{39c}$$

and

$$A = \pi r^2 \tag{40a}$$

$$Z_x = \frac{4}{3} r^3 \tag{40b}$$

$$Z_y = \frac{4}{3} r^3 \tag{40c}$$

Using Eqs. (39) and (40), the corresponding expressions for a hollow circular section of external radius r_o and internal radius r_i can be obtained (Fig. 8)

$$A_p = A_p(r_o) - A_p(r_i) \tag{41a}$$

$$Q_x = Q_x(r_o) - Q_x(r_i) \tag{41b}$$

$$Q_y = Q_y(r_o) - Q_y(r_i) \tag{41c}$$

and

$$A = \pi\,(r_o^2 - r_i^2) \tag{42a}$$

$$Z_x = \frac{4}{3}\,(r_o^3 - r_i^3) \tag{42b}$$

$$Z_y = \frac{4}{3}\,(r_o^3 - r_i^3) \tag{42c}$$

5. NUMERICAL RESULTS

Figures 9, 10 and 11 show numerical results for a wide-flange section, a double web section, and a hollow circular section, respectively. Referring to curves for the wide-flange section, W 14x426 (Fig. 9), the solid lines represent present exact solutions and the dotted lines are the results reported previously by Santathadaporn and Chen [1]. It is seen that they are practically identical to each other except in a small region. This small difference results from the fact that in Ref. 1 it is assumed that the N.A. cuts through the web horizontally as shown in Fig. 12a.

Furthermore, in Ref. 1 the cases where the N.A. cuts through an edge of the flange plate was omitted (Fig. 12a). As a consequence, a sharp corner appears on each of the interaction curves. Such corners do not show up on the exact interaction curves as one can see in the figure.

It should be noted that the present solution is exact only for the idealized wide-flange shape (Fig. 12b). An actual wide-flange shape has, of course, rounded corners and edges (Fig. 12c), not accounted for in this paper. Hence, emphasis must not be put on its exactness, rather, on its simplicity in calculations.

6. SIMPLE INTERACTION EQUATIONS FOR WIDE-FLANGE SECTIONS

In order to handle the interaction relation analytically, simple interaction equations are required. As a general form of the interaction equation, assume

$$\frac{m_x^{\alpha}}{1 - p^{\beta}} + \frac{m_y^{\mu}}{1 - p^{\nu}} + p^{\gamma} = 1 \qquad (44)$$

where α, β, γ, μ and ν are constants to be determined from the exact interaction relation. For most wide-flange sections, it is found that good agreement results when $\mu = 1$ and $\nu = \infty$.

When the strong axis bending moment M_x is large, the weak axis bending moment M_y has little effect on the interaction as shown in Fig. 9. Hence, the following two equations are assumed as the interaction equations for wide-flange sections

$$f_1 (m_x,m_y,p) = \frac{m_x^{\alpha}}{1 - p^{\beta}} + m_y + p^{\gamma} - 1 = 0$$

$$f_2 (m_x,m_y,p) = m_x + d^{\delta} - 1 = 0 \tag{45}$$

The actual interaction equation, $f (m_x,m_y,p)= 0$, is given by

$$f = f_1 (m_x,m_y,p) \qquad (\text{when} \quad m_y \geq \overline{m}_y)$$

$$f = f_2 (m_x,m_y,p) \qquad (\text{when} \quad m_y \leq \overline{m}_y) \tag{46}$$

and

$$\overline{m}_y = 1 - p^{\gamma} - \frac{(1 - p^{\delta})^{\alpha}}{1 - p^{\beta}} \tag{47}$$

The four constants, α, β, γ and δ, are determined using values of p, m_x and m_y corresponding to four representative points in the exact interaction relation.

As examples, the interaction curves for two wide-flange sahpes W8x31 and W14x426 were calculated and shown in Fig. 13 and

Fig. 14, respectively. The solid lines show the exact solutions and the dotted lines are results using the simple interaction equations (Eq. (46)). The approximation is seen to be quite good. In the figures, the four points indicated by the circles are the selected exact points. Their numerical values and the corresponding four constants are as follows:

W8x31

$$
\begin{array}{lll}
p_1 = 0 & m_{x1} = 0.34 & m_{y1} = 0.93 \\
p_2 = 0.7 & m_{x2} = 0 & m_{y2} = 0.62 \\
p_3 = 0.6 & m_{x3} = 0.22 & m_{y3} = 0.70 \\
p_4 = 0.4 & m_{x4} = 0.69 & m_{y4} = 0
\end{array}
$$

and

$$\alpha = 2.453, \quad \beta = 1.209, \quad \gamma = 2.714, \quad \delta = 1.987 \qquad (48a)$$

W14x426

$$
\begin{array}{lll}
p_1 = 0 & m_{x1} = 0.31 & m_{y1} = 0.92 \\
p_2 = 0.7 & m_{x2} = 0 & m_{y2} = 0.59 \\
p_3 = 0.6 & m_{x3} = 0.23 & m_{y3} = 0.66 \\
p_4 = 0.4 & m_{x4} = 0.71 & m_{y4} = 0
\end{array}
$$

and

$$\alpha = 2.176, \quad \beta = 2.678, \quad \gamma = 2.480, \quad \delta = 1.357 \qquad (48b)$$

7. FORCE-DEFORMATION RATE RELATIONS

The analytical description of the interaction relations given in the preceding section may be considered as a suitable basis for a three-dimensional space frame analysis. With this concept, the interaction surface (Eq. (45)) is assumed to be the perfectly plastic yield surface, and the force-deformation rate relations can then be derived from the normality condition (flow rule).

Thus, if $f\,(m_x, m_y, p) = 0$ denotes the yield condition, with $f < 0$ corresponding to stress states below yield, then

$$\dot{\kappa}_x = \lambda \left. \frac{\partial f}{\partial m_x} \right/ M_{px} \tag{49a}$$

$$\dot{\kappa}_y = \lambda \left. \frac{\partial f}{\partial m_y} \right/ M_{py} \tag{49b}$$

$$\dot{\varepsilon}_o = \lambda \left. \frac{\partial f}{\partial p} \right/ P_y \tag{49c}$$

If either (i) $f < 0$ or (ii) $f = 0$ and $\dot{f} < 0$

$$\dot{\kappa}_x = \dot{\kappa}_y = \dot{\varepsilon}_o = 0 \tag{50}$$

where λ is a positive scalar.

According to the concept of perfect plasticity, the vector representing the deformation rate is normal to the yield surface at a regular point. At a singular point of the yield surface, the deformation rate vector lies within the directions of the normals to the surface at adjacent points. For example, the normals drawn to the curve AB and line BC in Fig. 15 are the projections on the plane p = constant of Fig. 15 of possible deformation rates for stress points lying on curve AB and line BC. When the stress point lies at the corner B in Fig. 15, the deformation rate vector lies in the fan bounded by the normals to the sides which meet at the corner.

For the face AB of the yield surface, $m_y > \overline{m}_y$

$$\dot{\kappa}_x = \frac{\lambda}{M_{px}} \frac{\alpha}{1 - p^\beta} m_x^{\alpha-1} \tag{51a}$$

$$\dot{\kappa}_y = \frac{\lambda}{M_{py}} \tag{51b}$$

$$\dot{\epsilon}_o = \frac{\lambda}{P_y} \left[\frac{\beta p^{\beta-1}}{(1 - p^\beta)^2} m_x^\alpha + \gamma p^{\gamma-1} \right] \tag{51c}$$

where $\overline{m}_y$ is the value at the edge of the yield surface as given by Eq. (47).

For the face BC of the yield surface, $m_y < \overline{m}_y$

$$\dot{\kappa}_x = \frac{\lambda}{M_{px}} \tag{52a}$$

$$\dot{\kappa}_y = 0 \tag{52b}$$

$$\dot{\epsilon}_o = \frac{\lambda}{P_y} \delta p^{\delta-1} \tag{52c}$$

At the edge B of the yield surface, $m = \overline{m}_y$, it is convenient to introduce a scalar parameter ρ ($0 \leq \rho \leq 1$ at most) of position and time whose increase corresponds to a transition between the regular faces reckoned in a counter-clockwise sense round the yield curve CBA.

$$\dot{\kappa}_x = \frac{\lambda}{M_{px}} \left[1 - \rho + \frac{\alpha}{1 - p^\beta} m_x^{\alpha-1} \rho \right] \tag{53a}$$

$$\dot{\kappa}_y = \frac{\lambda}{M_{py}} \rho \tag{53b}$$

$$\dot{\epsilon}_o = \frac{\lambda}{P_y} \left[\frac{\beta p^{\beta-1}}{(1 - p^\beta)^2} m_x^\alpha \rho + \gamma p^{\gamma-1} \rho + \delta p^{\delta-1} (1 - \rho) \right] \tag{53c}$$

8. CONCLUSIONS

A simple method has been presented to arrive at the exact interaction relation of doubly symmetric sections under combined axial force and biaxial bending moments. The exactness of the solution is checked by the upper and lower bound limit analyses. Simple interaction equations of wide-flange sections are proposed and their associated plastic deformation rates are derived.

9. REFERENCES

1. Santathadaporn, S. and Chen, W. F.
   INTERACTION CURVES FOR SECTIONS UNDER COMBINED BIAXIAL BENDING AND AXIAL FORCE, Welding Research Council Bulletins No. 148, February 1970.

2. Morris, G. A. and Fenves, S. J.
   APPROXIMATE YIELD SURFACE EQUATIONS, Journal of the Engineering Mechanics Division, ASCE, No. EM4, August 1969.

10. NOTATIONS

A, A_i	= areas
A_p	= area contributing to axial force
b, b_o, b_1, b_2, B	= widths (Fig. 6)
d, d_o, d_1, D	= depths (Fig. 6)
e, e_{xi}, e_{yi}	= distances (Fig. 5)
M_x, M_y	= bending moments
M_{px}, M_{py}	= plastic moments
m_x, m_y	= M_x/M_{px}, M_y/M_{py}
P	= axial force
P_y	= axial force at yielding
p	= P/P_y
Q_x, Q_y	= static moments of section
r, r_o, r_i	= radii
S_x, S_y	= elastic section moduli
t_f, t_w	= thickness (Fig. 6)
Z_x, Z_y	= plastic section moduli
$\alpha, \beta, \lambda, \delta, \mu, \nu$	= constants
$\dot{\epsilon}, \dot{\epsilon}_o$	= rates of strain
$\dot{\kappa}, \dot{\kappa}_x, \dot{\kappa}_y$	= rates of curvature
σ_y	= yield stress
θ	= angle between N.A. and x-axis (Fig. 1)
η	= distance from N.A.

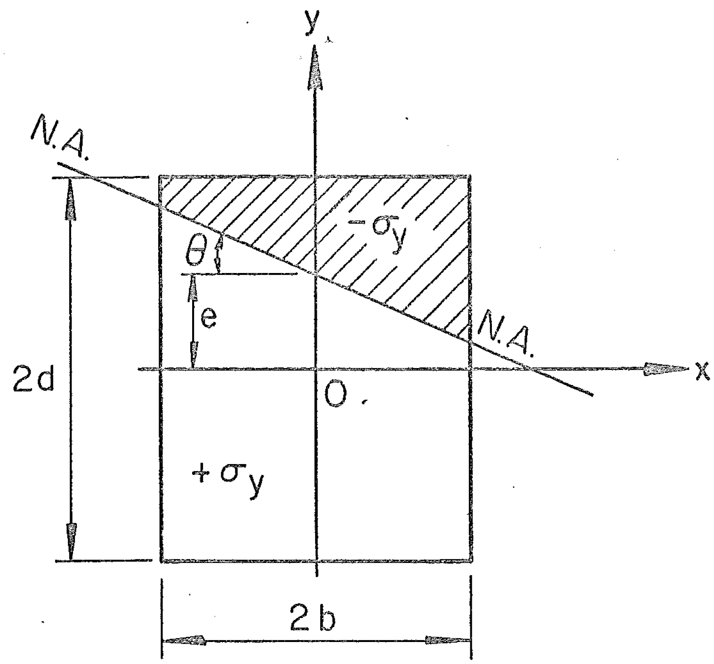

Fig. 1 Rectangular Section and Neutral Axis

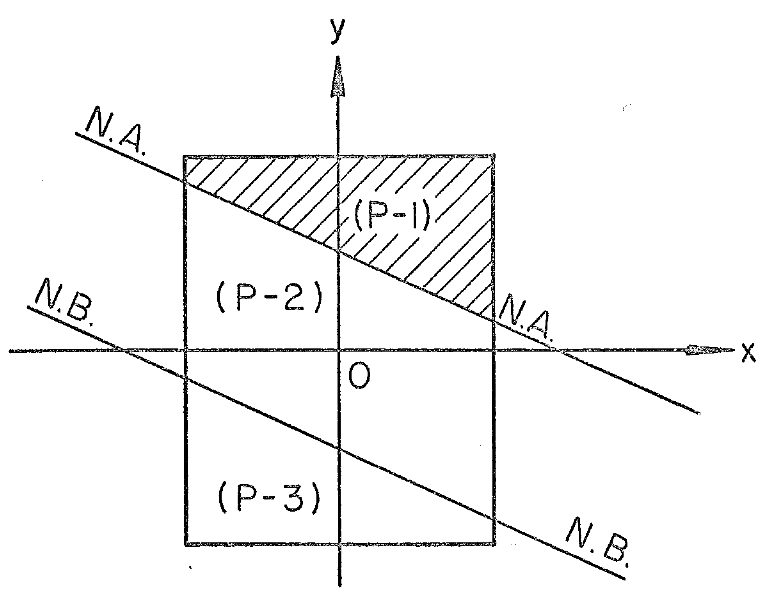

Fig. 2 Partitioning of Rectangular Section

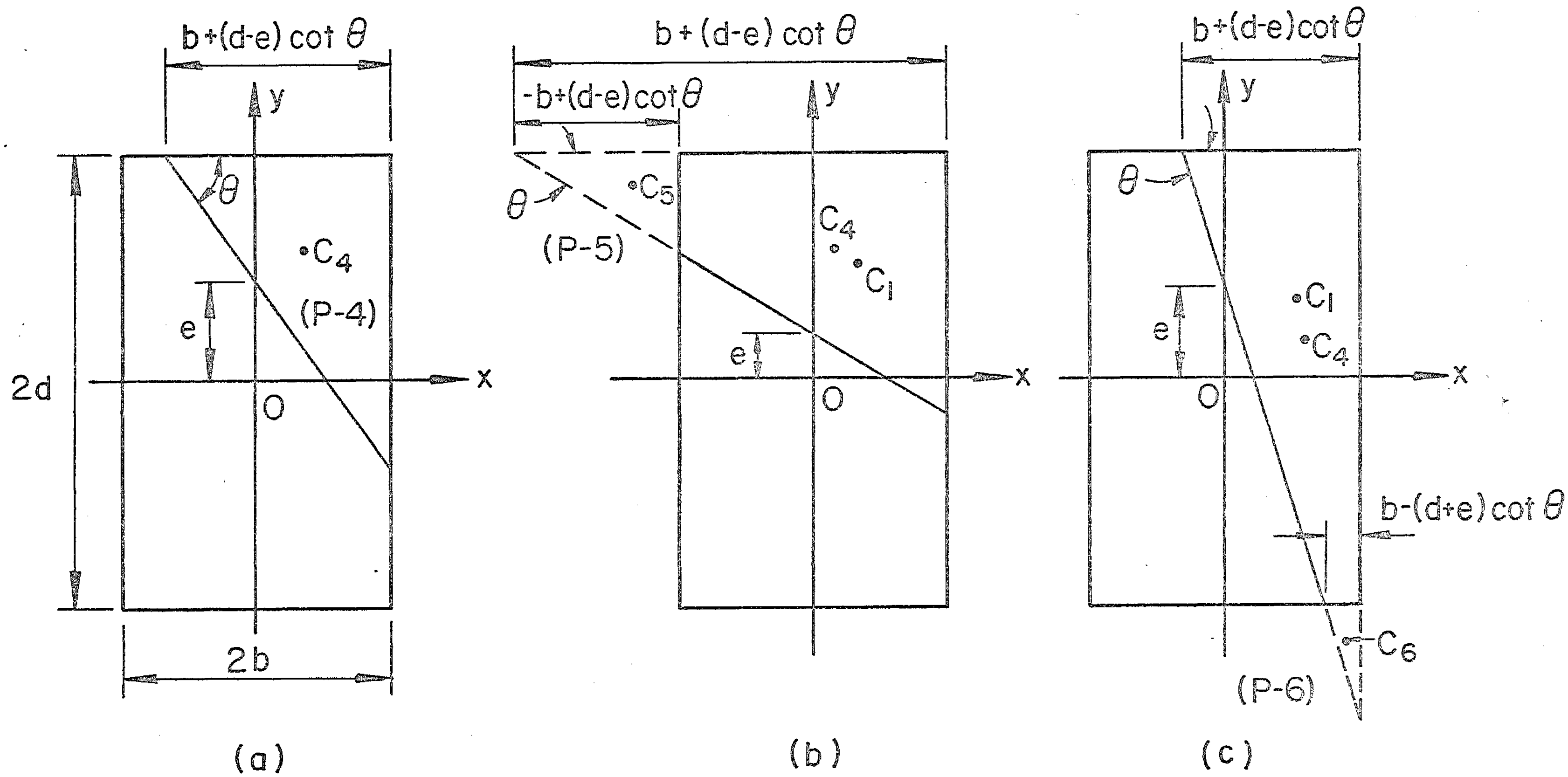

Fig. 3 Possible Locations of Neutral Axis

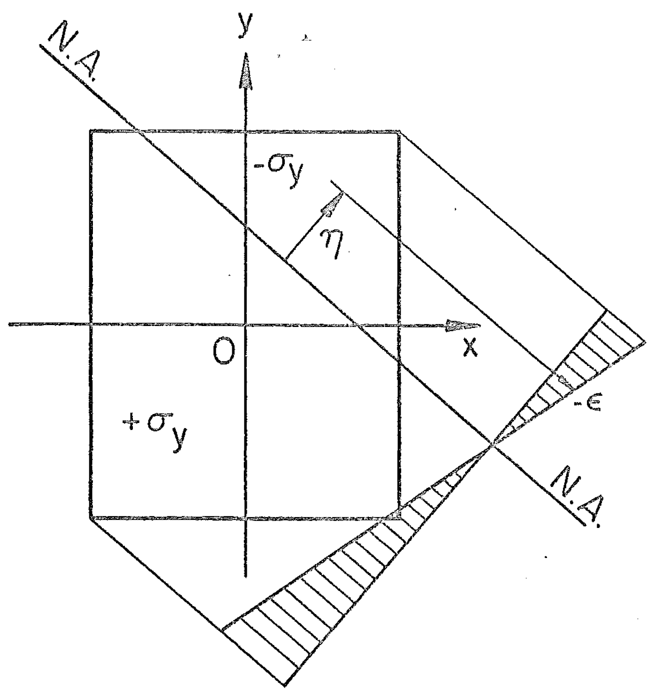

Fig. 4 Distribution of Strain Rate

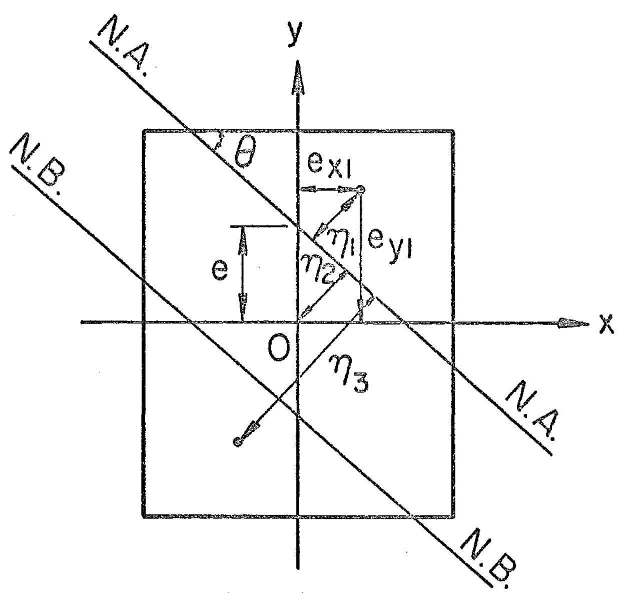

Fig. 5 Geometry of Centroidal Points

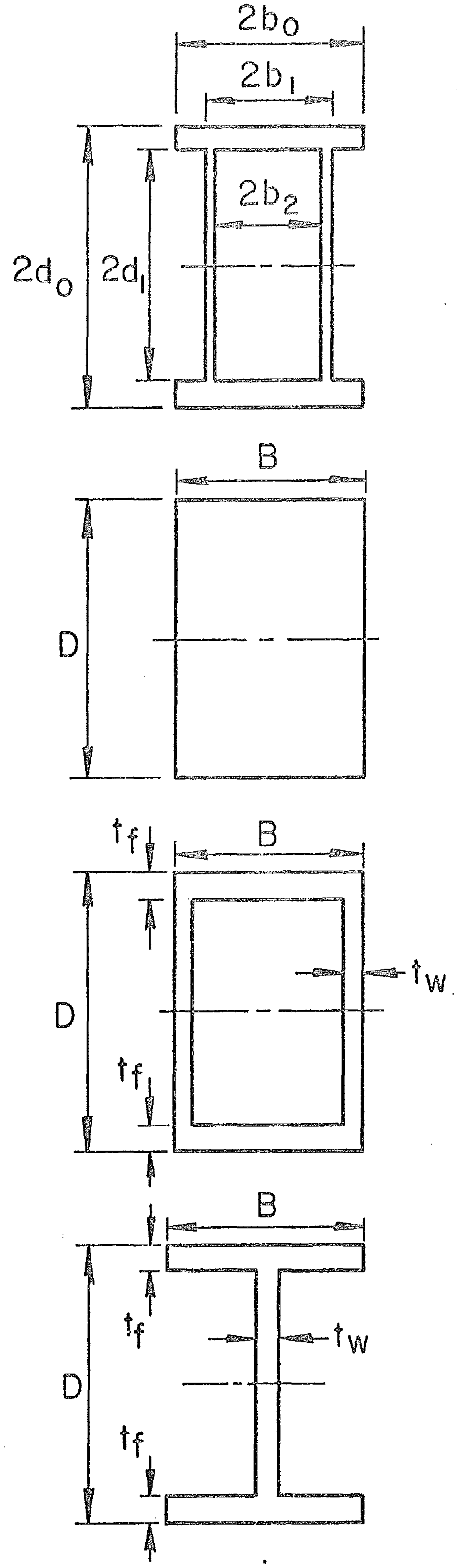

Double Web Section

Rectangular Section

$b_0 = b_1 = \frac{1}{2} B, \quad b_2 = 0$

$d_0 = \frac{1}{2} D, \quad d_1 = 0$

Box Section

$b_0 = b_1 = \frac{1}{2} B, \quad b_2 = \frac{1}{2} B - t_w$

$d_0 = \frac{1}{2} D, \quad d_1 = \frac{1}{2} D - t_f$

Wide Flange Section

$b_0 = \frac{1}{2} B, \quad b_1 = \frac{1}{2} t_w, \quad b_2 = 0$

$d_0 = \frac{1}{2} D, \quad d_1 = \frac{1}{2} D - t_f$

Fig. 6 Particular Cases of Double Web Section

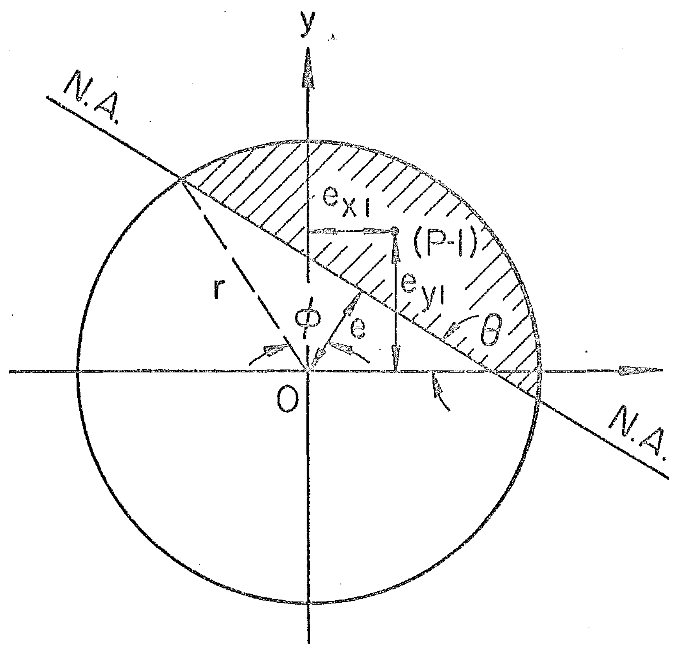

Fig. 7 Solid Circular Section

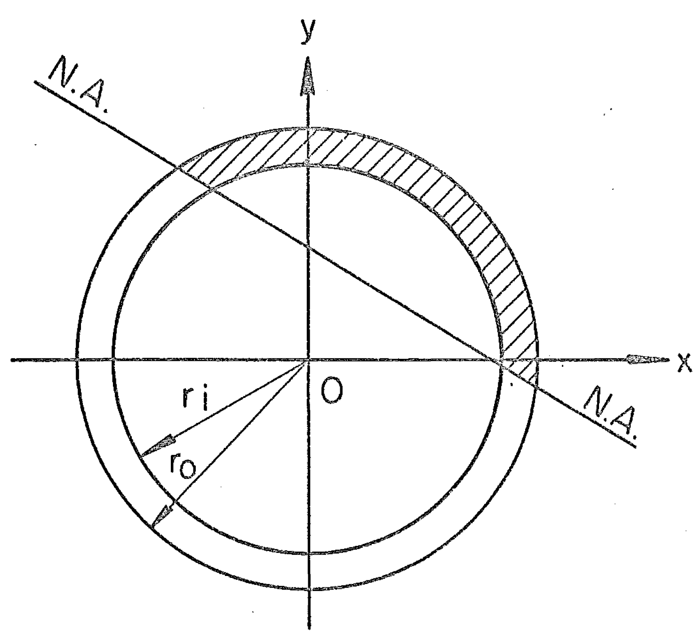

Fig. 8 Hollow Circular Section

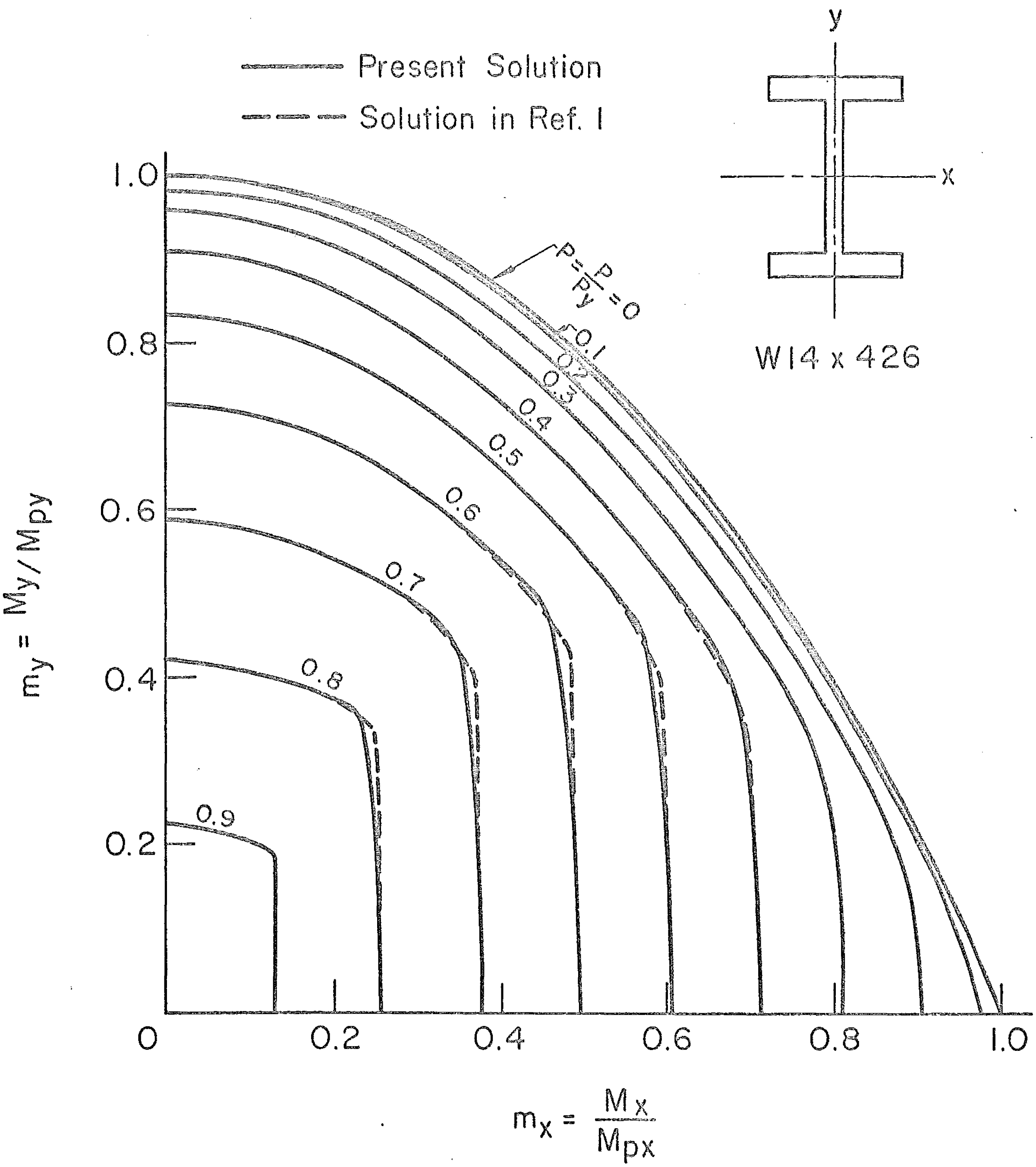

Fig. 9 Interaction Curves for a Wide Flange Section

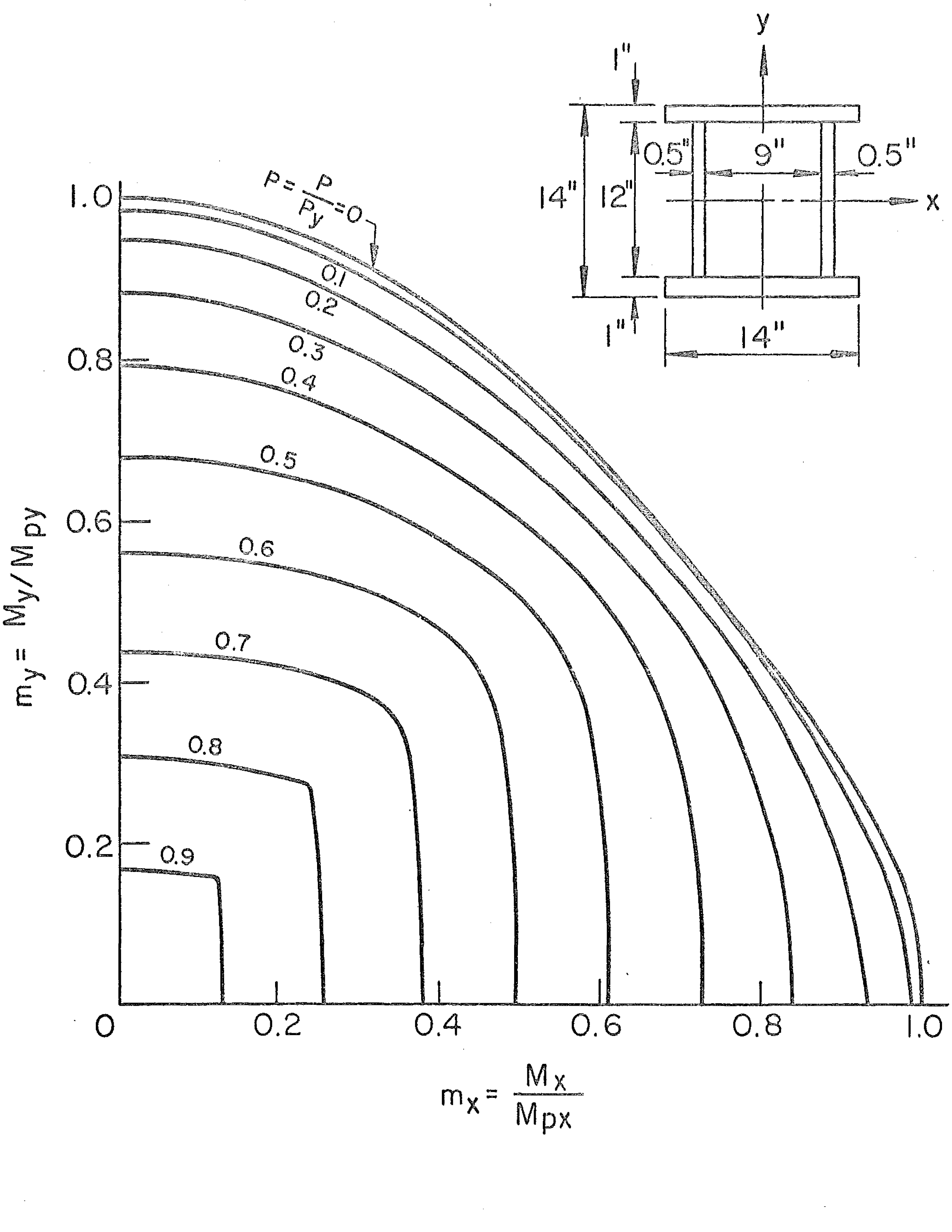

Fig. 10 Interaction Curves for a Double Web Section

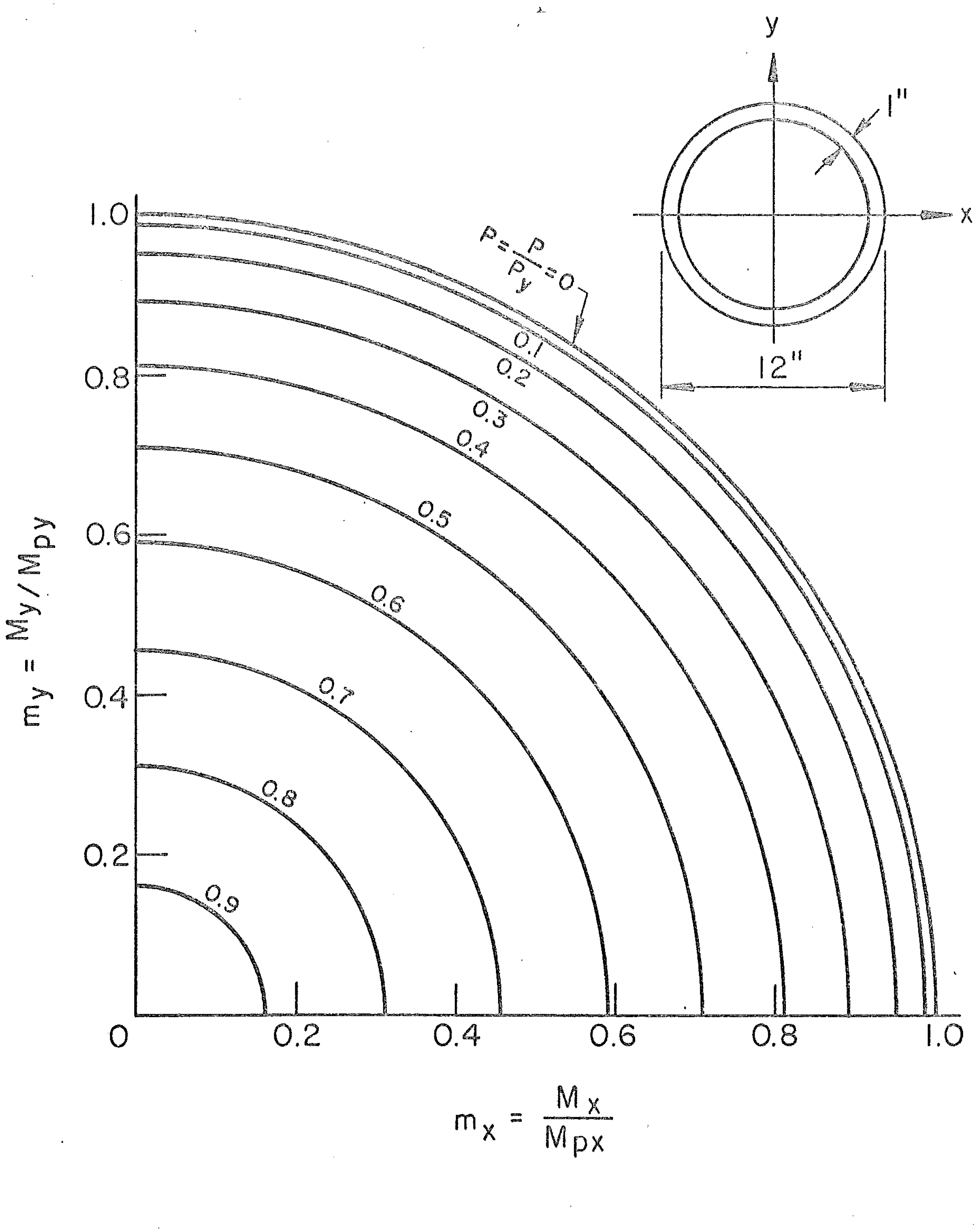

Fig. 11 Interaction Curves of a Hollow Circular Section

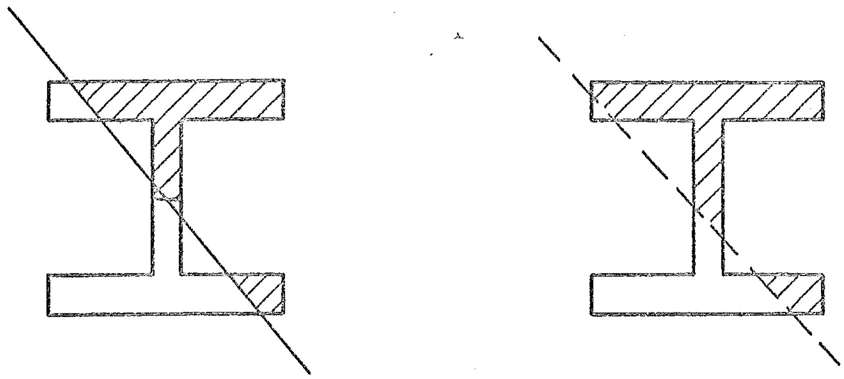

(a) Idealized Section with Approximate N.A. (Ref. 1)

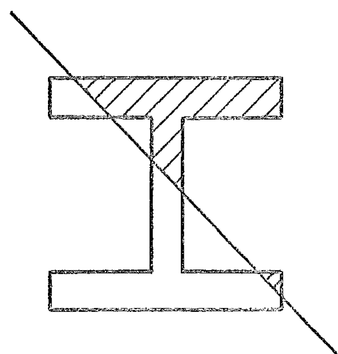

(b) Idealized Section with Exact N.A. (Present Solution)

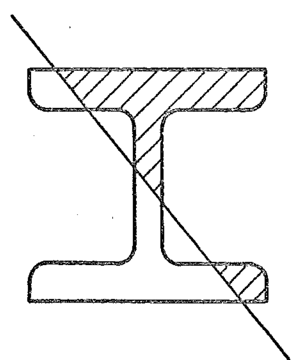

(c) Actual Section with Exact N.A.

Fig. 12 Wide Flange Sections and Neutral Axes

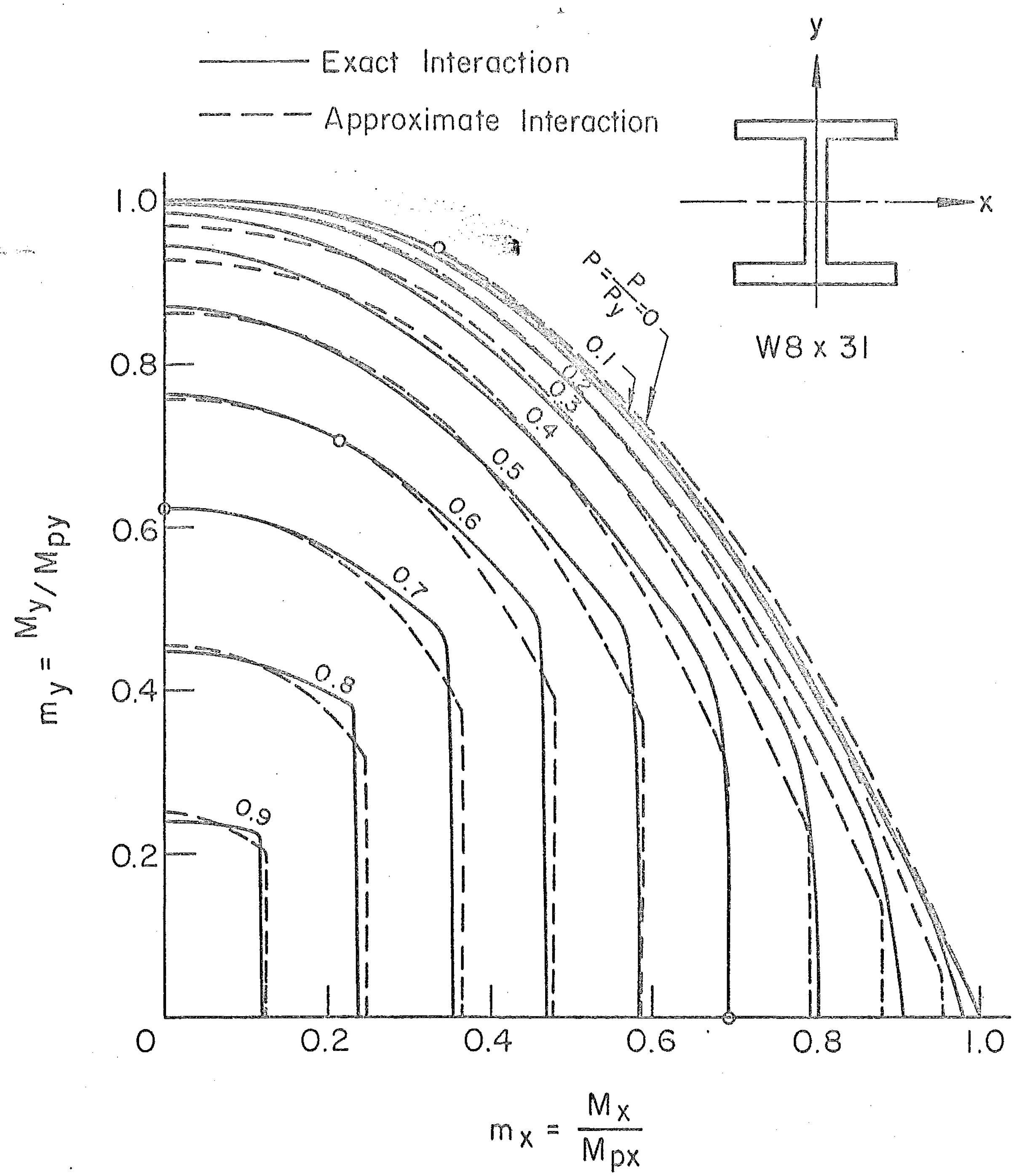

Fig. 13 Interaction Curves of Wide Flange Section

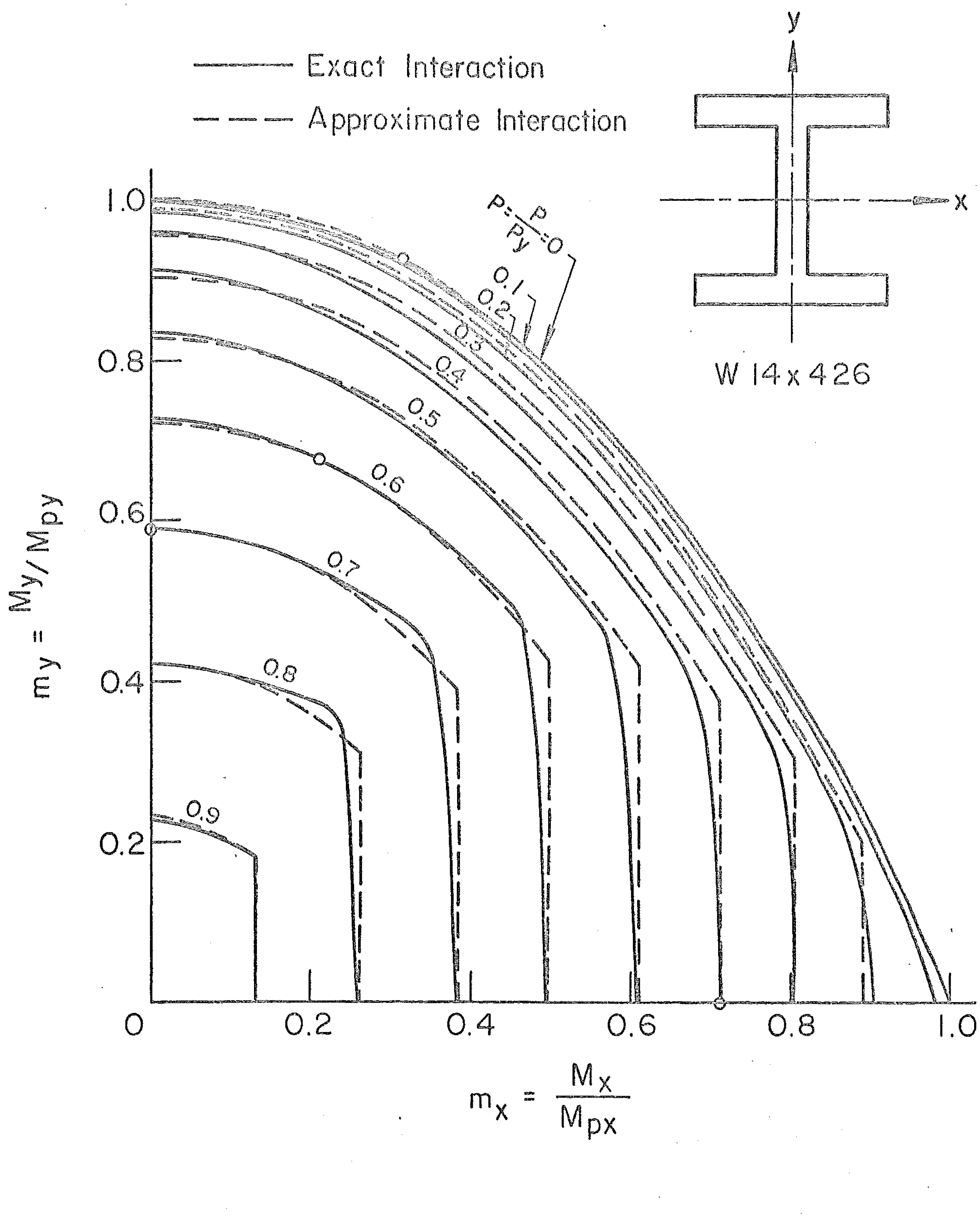

Fig. 14 Interaction Curves of Wide Flange Section

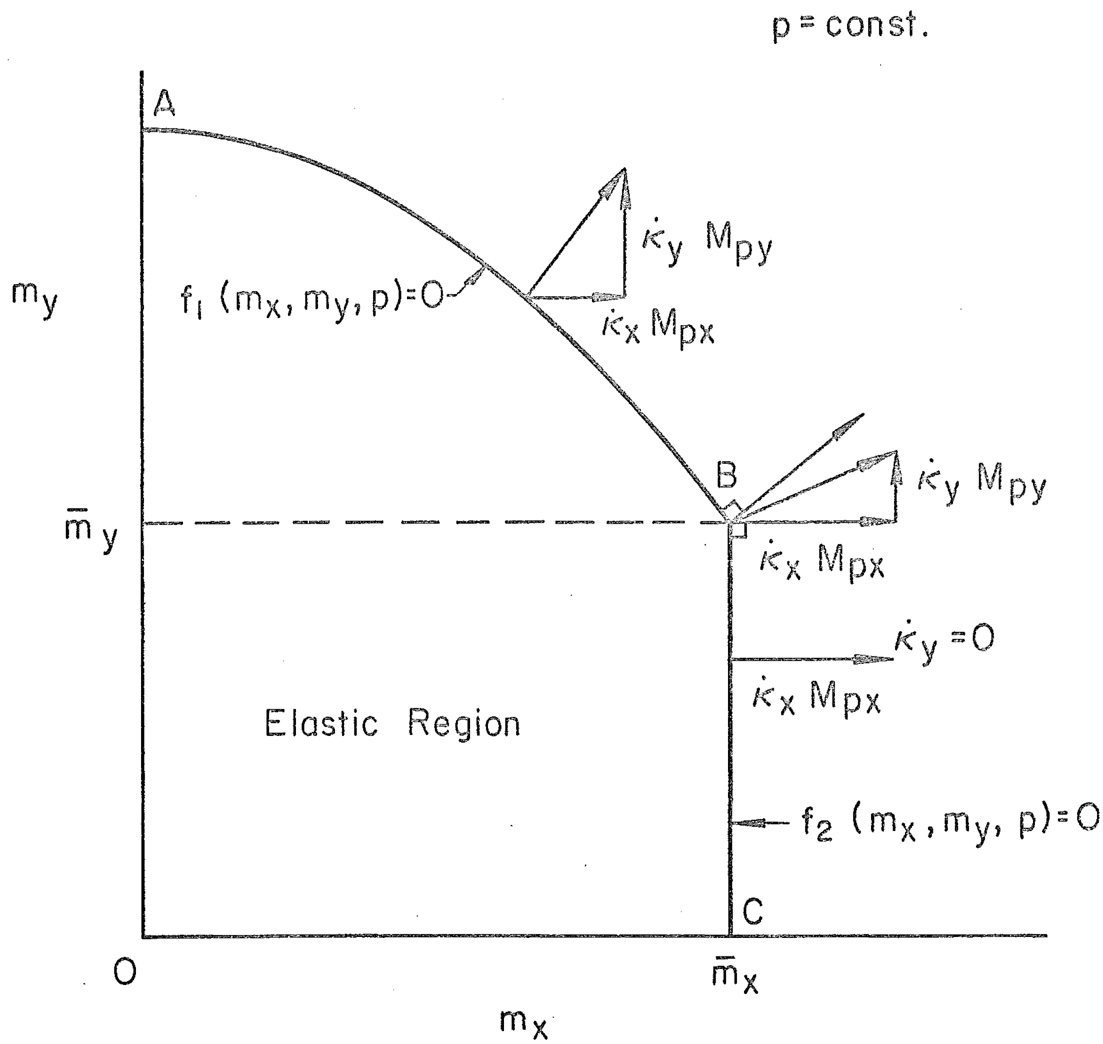

Fig. 15 Yield Surface and Strain Vectors